Chemical Physics Letters 743 (2020) 137184

Contents lists available at ScienceDirect

Chemical Physics Letters

journal homepage: www.elsevier.com/locate/cplett

Research paper

Structural, electronic, elastic and thermodynamic properties of hydrogen storage magnesium-based ternary hydrides

Selgin Al[a,*], Ahmet Iyigor[b]

[a] Department of Environmental Protection Technologies, Vocational School, Izmir Democracy University, 35140 Izmir, Turkey
[b] Machine and Metal Technologies, Vocational School of Technical Sciences, Ahi Evran University, 40100 Kirsehir, Turkey

HIGHLIGHTS

- Two new perovskite hydrates have been investigated for hydrogen storage.
- The electronic analysis showed that both hydrides are metallic.
- Both ternary hydrides are ductile in nature.

ARTICLE INFO

Keywords:
Hydrogen storage
First principle calculations
Electronic properties
Mechanical stability

ABSTRACT

In this study, new, lightweight perovskite type hydrides; $MgNiH_3$ (GHD is calculated as ~3.51 wt%) and $MgCuH_3$ (GHD is calculated as ~3.32 wt%) are investigated. Hydrogen storage, structural, elastic, mechanical, electronic and thermodynamic behaviour of these hydrides are investigated using first principle calculations as a tool. Our elastic and mechanical analysis revealed that these hydrides are mechanically stable and have a ductile nature which is a necessary assessment required for handling materials for transportation. Furthermore, electronic band structures of hydrides indicate metallic characteristics for both hydrides. Many unknown thermodynamic properties of these ternary hydrides are revealed and discussed.

1. Introduction

Magnesium hydride is a superior candidate for solid state hydrogen storage owing to its high volumetric and gravimetric hydrogen density (H_2 content in MgH_2 is 7.6 wt%) and its light weight specifically for automotive industry [1,2]. Moreover, magnesium is abundant in Earth's surface composition (~2.5%), non-toxic, safe (compared to alkaline metals which undergo violent reactions under oxidising conditions) and its production industry is well established [3]. However, magnesium shows slow kinetics of adsorption/desorption, high thermodynamic stability and strong bonding between magnesium and hydrogen [2]. These obstacles have been tried to overcome by particle size reduction, which led to reduction of hydrogen pathways, or addition of additivities such as transition metals that led to improvement of adsorption and desorption kinetics [4]. Decreasing the equilibrium temperature of desorption means lowering the thermodynamic enthalpy which can be managed by magnesium alloys formation. Significant progress has been made by researchers by tuning thermodynamic and kinetic properties of magnesium based hydrides to meet practical application criteria. Recent investigations focus on addition of 3d transition metals to magnesium based hydrides which seems to be a progress for solid state hydrogen storage without sacrificing too much hydrogen storage capacity. Mg-Ni and Mg-Cu binary alloys have shown promising progress and studied extensively [5,6]. $Mg_{1-x}Ni_x$ alloys were prepared with various compositions ($0 \leq x \leq 0.33$) using melt-spinning method and seen an increasing hydrogen sorption kinetics with Ni [7]. Moreover, Ni seems to destabilize Mg-H bonding thus reducing the dehydrogenation temperature [4]. Recently, Mg-Ni and Mg-Cu nano-powders were successfully prepared using physical vapour deposition method and phase formations were verified [8]. The impact of ball milling on hydrogenation properties of binary Mg-Cu system was also investigated and reported an activated reversible hydrogenation reaction with reduced particle size [9]. Hydrating and dehydrating processes of Mg-Ni was studied using thermogravimetric analysis [10]. The search for Mg-based systems for better and practical hydrogen storage materials led research to ternary hydrides due to higher hydrogen content compared to alloy hydrides. There are few studies exist on ternary hydrides in literature. The formation enthalpies of various ternary hydrides in perovskite form

* Corresponding author.
E-mail address: selgin.al@idu.edu.tr (S. Al).

https://doi.org/10.1016/j.cplett.2020.137184
Received 17 January 2020; Received in revised form 2 February 2020; Accepted 4 February 2020
Available online 05 February 2020

($MgTMH_3$ hydrides, where TM = Sc, Ti, V, Cr, Mn, Fe, Co, Ni, Cu, Zn) were calculated by Vegge et al. [2] and it was shown that these hydrides are thermodynamically favourable and synthesisable. $MMgH_3$ (M = Na, K, Rb) perovskite hydrides were synthesised using ball milling method [11]. The structural and electronic properties of $MMgH_3$ (M = Li, Na, K, Rb, Cs) were investigated using first principle calculations [12,13]. The vibrational and structural properties of $AMgH_3$ (A = Na, K, Rb) hydrides in cubic form was studied by Fornari et al. [14]. Even tough, there are extensive studies on Mg-Ni and Mg-Cu binary alloys, experimental and theoretical investigations about fundamental properties of Mg-based ternary hydrides are scarce. In order to take full advantage of Mg-based hydrogen storage hydrides; structural, electronic, elastic and thermodynamic investigations are necessary. Therefore, this study adopts theoretical interpretation of Mg-based ternary hydrides, their structures, electronic, elastic and thermodynamic properties using computational methods. Special attention will be paid to $MgNiH_3$ (gravimetric hydrogen density is calculated as ~3.51 wt%) and $MgCuH_3$ (gravimetric hydrogen density is calculated as ~3.32 wt%) perovskite type hydrides. The mechanical, electronic and thermodynamic properties of those ternary hydrides will be discussed. The stability of hydrides will be examined using elastic constants.

2. Method

Density functional theory was utilised to run calculations in this study [15,16]. Quantum-Espresso software package was used to compute minimum energy, equilibrium volumes and structural properties [17]. Perdew-Burke-Ernzerhof, generalised gradient approximation (PBE-GGA) was utilized for the exchange correlation potential [18]. All elements' pseudopotentials were adopted from the Rappe group [19]. Brillouin zone integration was carried out using a 8 × 8 × 8 k-point mesh. The cut off energy was taken as 40 Ry for the expansion of electronic wave functions. The kinetic energy was set to 400 Ry for evaluation of electronic charge density. Methfessel-Paxton smearing method was adopted to carry out integration up to Fermi level with a smearing parameter of 0.02 Ry [20]. The lattice dynamic calculations were conducted using the density functional perturbation theory (DFPT) [21,22]. The materials' elastic constants were obtained from energy difference between distorted and undistorted lattice cell using the technique of stress-finite strain. The equations that were used to obtain elastic constants are given in [23,24]. Thermodynamic computations to get variables such as heat capacity, entropy were done using the Debye Model within Gibbs2 code described in [25].

3. Results and discussion

3.1. Structural and elastic properties

The ternary hydrides, $MgNiH_3$ and $MgCuH_3$, crystalize in an ideal perovskite structure with the space group $Pm\bar{3}m$ (no.221) as shown in Fig. 1. The structure has one formula per unit cell with the Wyckoff positions; magnesium (Mg) atoms are at the centre (1/2, 1/2, 1/2), Nickel (Ni)/Copper (Cu) atoms are at corners (0, 0, 0) and hydrogen (H) atoms are at (1/2, 0, 0) positions. The ground state properties of $MgNiH_3$ and $MgCuH_3$ ternary hydrides are obtained by computing total energies for various volumes around the equilibrium positions and then these results are fitted to Murnaghan's equation of state [26]. The structures of ternary hydrides are optimised in order to compute equilibrium lattice constants that are given in Table 1. The obtained results are compared to values that are available in literature [1,27]. The equilibrium lattice constants that are obtained in this study are in accordance with the previous results.

The elastic parameters of materials are crucial for understanding mechanical properties of compounds such as stability, anisotropic behaviour, internal forces, ductility and brittleness [28]. The elastic constants of a material (C_{ij}) defines its response towards an externally applied force. It shows the ability of material against deformation. For a

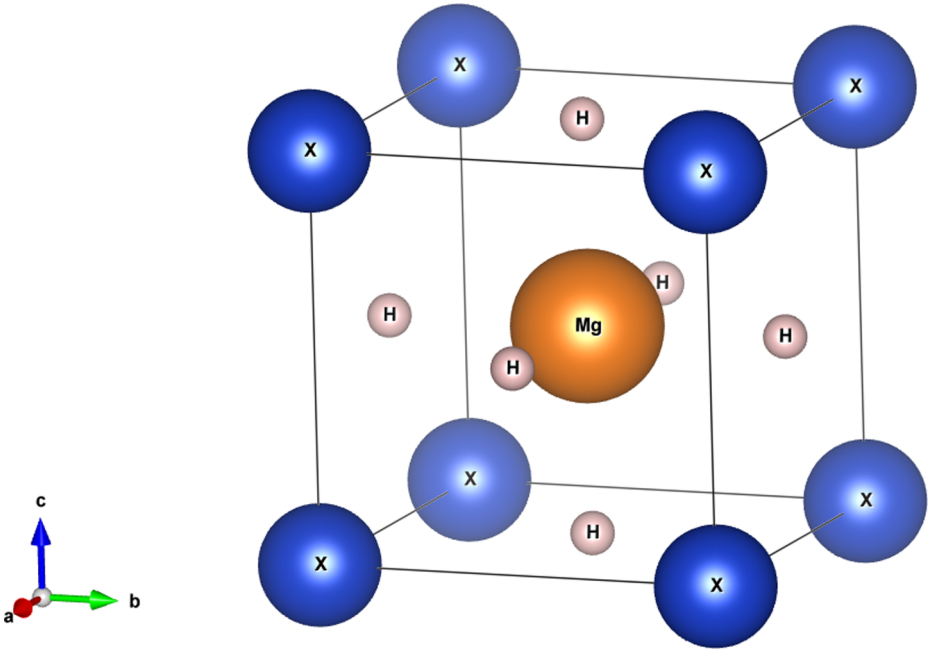

Fig. 1. Crystal structures of $MgNiH_3$ and $MgCuH_3$ (X = Ni or Cu).

Table 1
The calculated lattice constants (a), Bulk modulus (B), elastic constants (C_{11}, C_{12}, C_{44}) and Cauchy Pressures (C_P) of $MgNiH_3$ and $MgCuH_3$.

Materials	References	a	B	C_{11}	C_{12}	C_{44}	C_{12} - C_{44} (C_P)
$MgNiH_3$	This work	3.332	120.45	220.75	70.3	29.87	40.43
	Abdellaoui et al. [1]	3.37					
$MgCuH_3$	This work	3.456	86.87	110.86	74.13	4.63	69.5
	Matar et al. [27]	3.32					

cubic system as ours, there are three independent elastic constants exist; C_{11}, C_{12} and C_{44} which are presented in Table 1. C_{11} represents axial compression, C_{12} and C_{44} present shear modulus and dilation on compression, respectively. These constants define the mechanical stability of a material by [29];

$$(C_{11} - C_{12}) > 0, C_{11} > 0, C_{44} > 0, (C_{11} + 2C_{12}) > 0 \quad (1)$$

Eq. (1) also limits Bulk modulus as;

$$C_{12} < B < C_{11} \quad (2)$$

The obtained elastic constants of hydrides are all positive as can be seen from Table 1. These results are the first elastic constants of these materials presented in literature. From Table 1, one can easily see that both hydrides fulfil the stability criteria given in Eqs. (1) and (2). Therefore, it can be safely said that both ternary hydrides are mechanically stable. The unidirectional compression (along the x-axis) is represented by C_{11} [30]. As can be noticed from Table 1 that C_{11} values of both hydrides are much higher than that of C_{44}, indicating that the resistance against unidirectional compression is much higher compared to resistance shear deformation compression for both hydrides. Furthermore, the value of C_{11} is lower for $MgCuH_3$ than that of $MgNiH_3$, demonstrating that $MgCuH_3$ has weaker resistance against unidirectional compression than $MgNiH_3$ [31].

Elastic constant computation promotes understanding of fundamental, structural and mechanical properties of a material and allow one to obtain several polycrystalline elastic moduli given in Table 2. The computation detail of parameters are given in [31]. Bulk modulus of a material defines its response to a shape change under hydrostatic pressure. Hence, it can be adopted to measure average bong strength due to having a strong connection with cohesive energy or binding energies of atoms within the material. As higher bulk modulus gets, the higher the resistance becomes [32]. The bulk modulus of $MgNiH_3$ is higher compared to $MgCuH_3$. Shear modulus (G) of hydrides are obtained by using the Voigt Reus Hill approach where Reuss's shear modulus (G_R) is associated with lower value of G and the Voight's shear modulus (G_V) is associated with higher value of G. The G is defined as a ratio between shear stress and strain. From Table 2, it can be seen that shear modulus of $MgNiH_3$ is greater than that of $MgCuH_3$, indicating that $MgNiH_3$ will show higher resistance to shear deformation. This prediction is in accordance with B values. By comparing the two ternary hydrides, it can be predicted that $MgNiH_3$ has much rigid structure than $MgCuH_3$.

Another important parameter that is driven from Bulk and shear modulus is that the ratio of B/G. This ratio classifies materials as ductile or brittle based on the Pugh's criteria [33]. In the case of $B/G > 1.75$, the material has ductile nature, in other case, ($B/G < 1.75$) the material shows brittle nature [34]. From our results in Table 2, both hydrides have ductile nature. That is a critical parameter to determine practical hydrogen storage materials since it will eliminate handling problem especially for on-board applications. In addition to B/G values, C_P (Cauchy Pressure) given in Table 1 is used to understand ductility and brittleness of hydrides. C_P of hydrides can also be used to estimate angular characteristic of atomic bonding. A negative value of C_P means directional bonding with angular character and brittleness, on the other hand, a positive value of C_P means more metallic and ductile nature [35]. Based on the both B/G and C_P values, both hydrides have ductile and metallic nature.

Poisson's ratio (σ), provides insight about bonding nature of materials. As the value of σ gets higher, the plasticity of material increases [36,37]. If the value of σ is around 0.1, the material shows covalent characteristics, if it is around 0.25, the material shows ionic characteristic [38]. Also, it was reported that 0.5 and 0.25 are upper and lower limits for σ ratio for central force of a solid [30]. The σ values of both hydrides are between 0.5 and 0.25, demonstrating that both hydrides have dominant ionic nature and the forces are central.

Young Modulus (E) of a material is defined as the ratio of tensile stress to tensile strain. As E increases, the stiffness of the material increases [39]. Based on the results given in Table 2, it can be predicted that $MgNiH_3$ is the stiffest hydride with respect to $MgCuH_3$.

The elastic anisotropy is an another important parameter that is related with micro cracks, precipitation, anisotropic plastic deformation, elastic instability and internal friction [40,41]. If this value equals to one, the material is completely isotropic, deviation from this value exhibits the anisotropy degree. The elastic anisotropy factor can be computed using three independent elastic constants ($A = 2C_{44}/(C_{11} - C_{12})$.As Table 2 illustrates that both hydrides have anisotropy factors that are lower than 1, indicating an anisotropic nature. From the results in Table 2, $MgNiH_3$ has higher anisotropy compared to $MgCuH_3$. Due to the fact that both hydrides are not completely isotropic, 2D directional change of compressibility, Poisson's ratio, Shear and Young Modulus of $MgNiH_3$ and $MgCuH_3$ are calculated using EIAM code [42]. The results are given in Fig. 2. Fig. 2 illustrates that the compressibility of both hydrides are spherical whereas Poisson's ratio, Shear and Young Modulus of $MgNiH_3$ and $MgCuH_3$ display a deviation from isotropy and becomes anisotropic at all directions.

Table 2
The calculated Bulk modulus (B), Shear modulus (G), B/G ratios, anisotropy factor (A), Poisson's ratios (σ) and Young's modulus (E) of $MgNiH_3$ and $MgCuH_3$.

Materials	References	B	G	G_v	G_R	B/G	A	σ	E
$MgNiH_3$	This work	120.45	43.68	48.01	39.36	2.75	0.397	0.338	116.92
$MgCuH_3$	This work	86.87	8.363	10.124	6.606	10.38	0.252	0.453	24.31

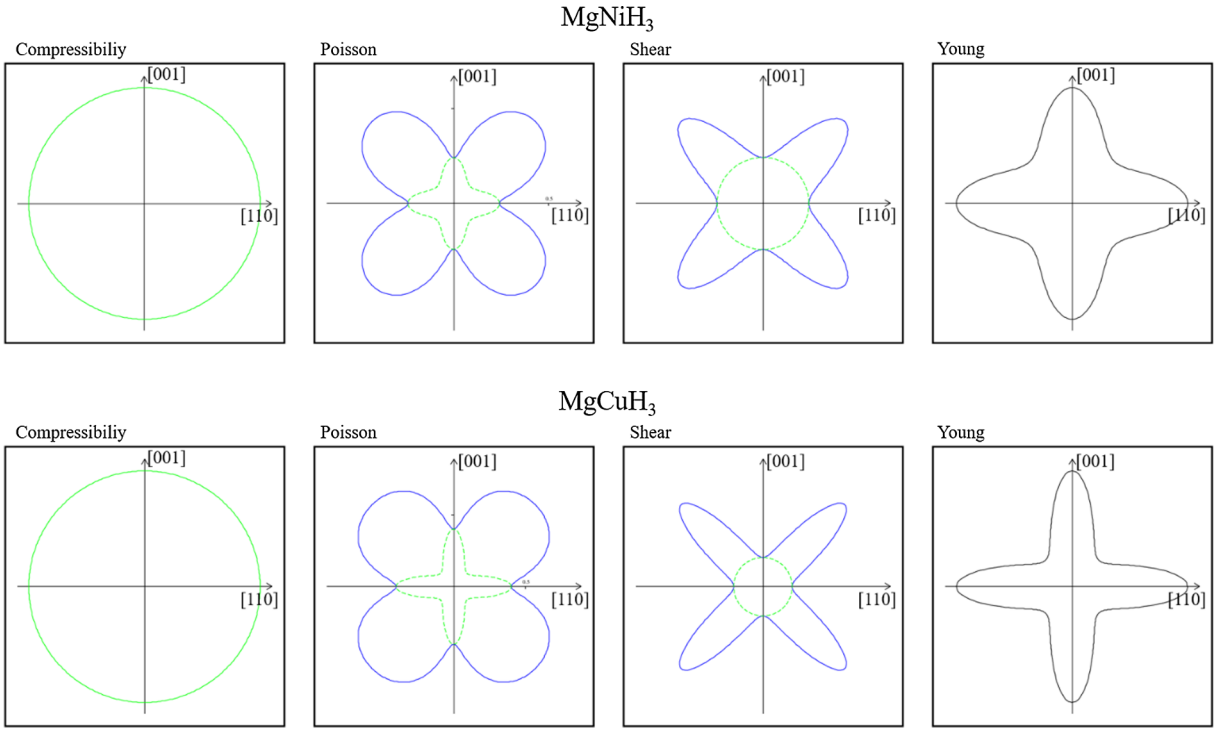

Fig. 2. 2D directional change of compressibility, Poisson's ratio, Shear and Young Modulus of $MgNiH_3$ and $MgCuH_3$.

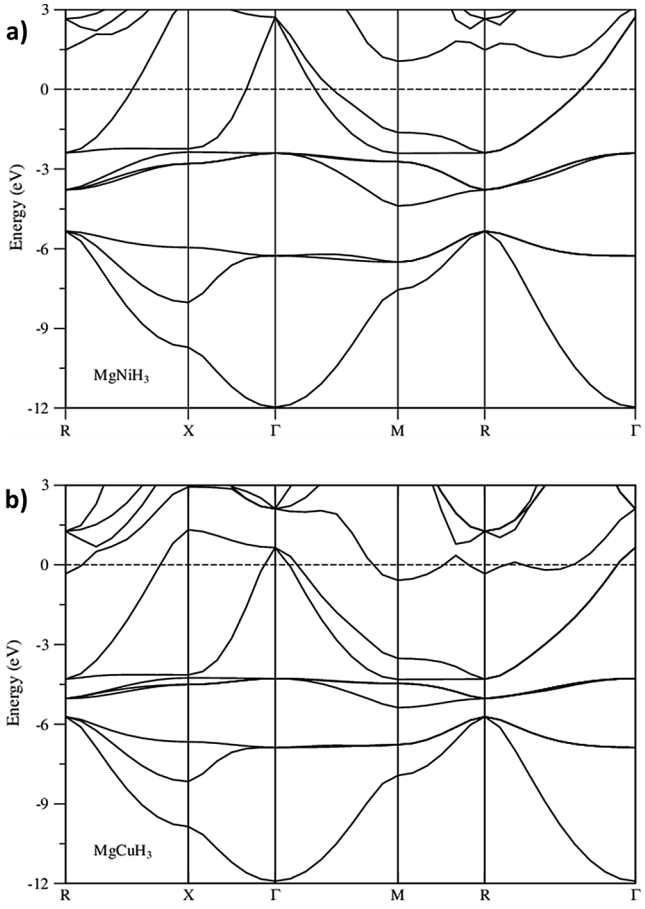

Fig. 3. Electronic band structures of $MgNiH_3$ and $MgCuH_3$.

3.2. Electronic properties

The obtained electronic band structure of hydrides along with the high symmetry directions are presented in Fig. 3. Fermi energy level is set to 0 eV. From Fig. 3, it can be seen that some bands cross Fermi energy level and there is no band gap exist, demonstrating metallic characteristic of both hydrides. In order to gain much insight into the electronic structures of hydrides and determine the contributions of each element to the metallicity, the total and partial density of states of $MgNiH_3$ and $MgCuH_3$ are computed and presented in Fig. 4. For $MgNiH_3$, in the energy range between -7 eV and -5eV below Fermi level, the biggest contribution to the conduction comes from the Ni-d states with a few contributions from Mg-p states. For $MgCuH_3$, Cu-d states are dominant at 4.5 eV energy level. At around Fermi level, most contributions are due to Ni-d and Cu-d states for $MgNiH_3$ and $MgCuH_3$.

3.3. Thermodynamic properties

The ground state properties of hydrides are used to obtain thermal properties such as entropy, specific heat values, thermal expansion coefficient and Grüneisen parameter using quasi-harmonic Debye model calculations within the temperature range of 0–1400 K. Debye temperature is an important parameter that defines heat capacity of solids. Debye temperatures of hydrides are found to be 418.38 K and 280.96 K for $MgNiH_3$ and $MgCuH_3$, respectively. Entropy of a system provides information about its thermal energy. Fig. 5 depicts calculated entropy change of $MgNiH_3$ and $MgCuH_3$ versus temperature. It is clear that the entropy is zero at 0 K. Then, it increases as temperature increases due to the fact that thermal vibrations of atoms increase as temperature increases.

The specific heat is another thermodynamic property which gives insight into heat loss or retention. The capacities of hydrides at a constant volume (C_v) and pressure (C_p) are presented in Fig. 6. As can be seen from Fig. 6 that both heat capacities increase rapidly from 0 K

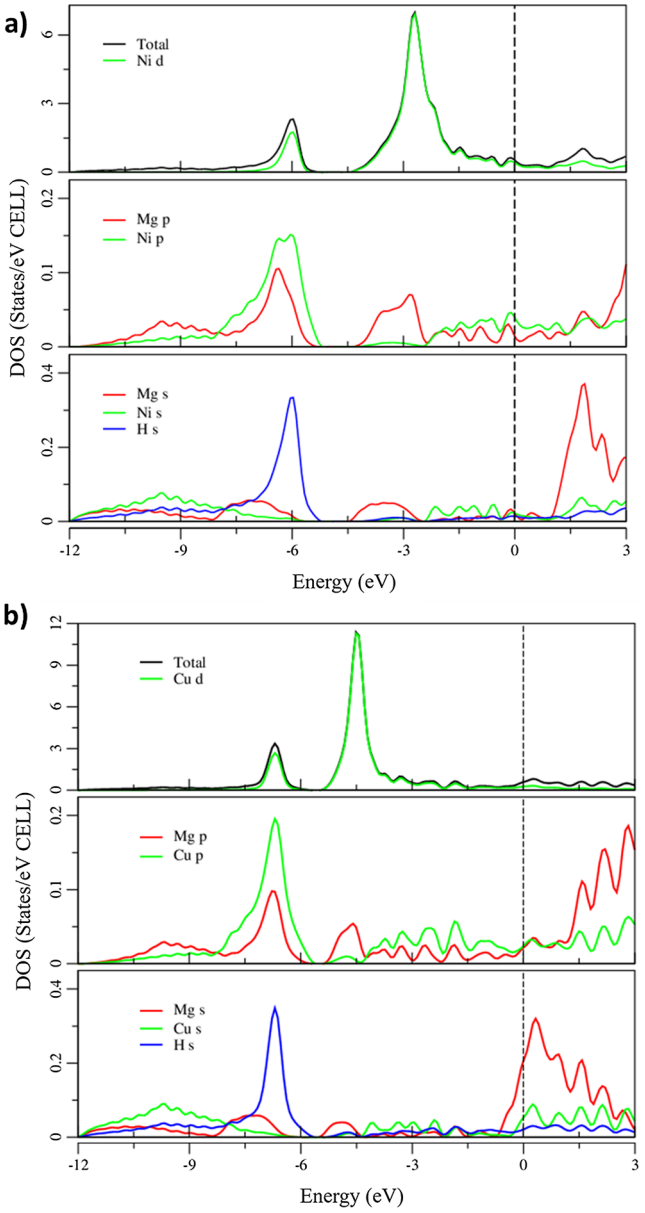

Fig. 4. The total and partial density of states of $MgNiH_3$ and $MgCuH_3$.

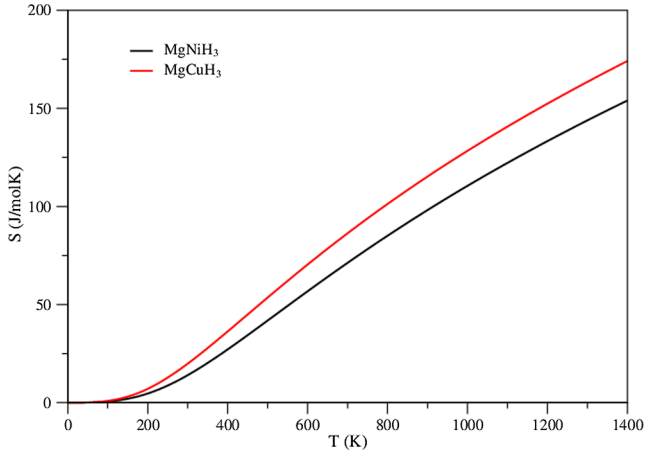

Fig. 5. Entropy change of $MgNiH_3$ and $MgCuH_3$ with temperature.

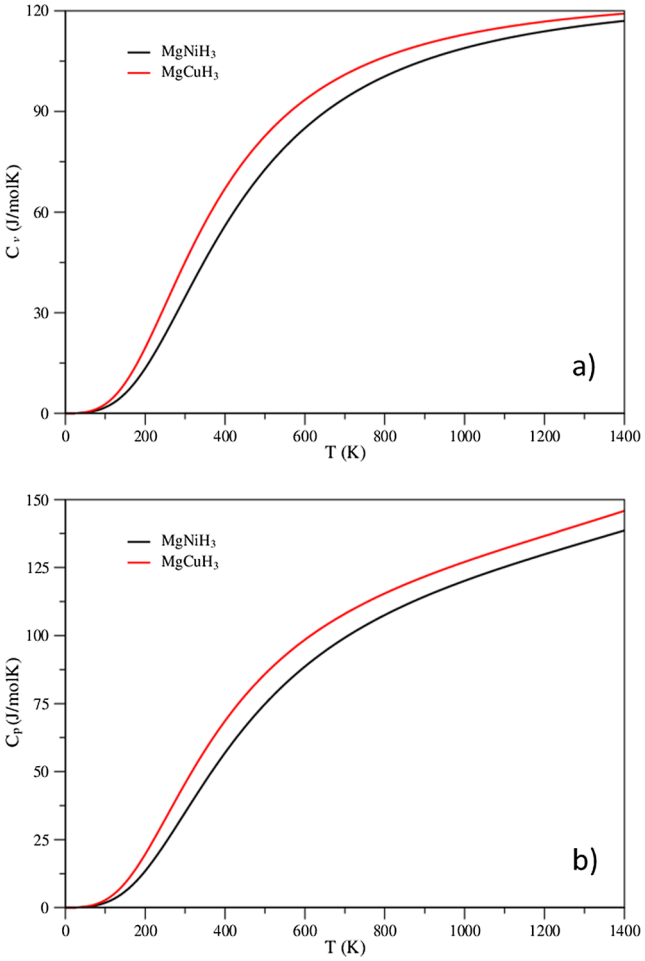

Fig. 6. The temperature dependence of the specific heat capacities at constant volume (C_v) (a) and pressure (C_p) (b) of $MgNiH_3$ and $MgCuH_3$.

to 700 K, then a sluggish increase continues up until 1300 K. And finally they are expected to reach Dulong-Petit limit [43] where a saturation limit occurs. The calculations in this study can serve as a reference data since there is no theoretical or experimental data exist with respect to thermodynamic properties for these hydrides up to date.

Thermal expansion coefficient (α) describes thermal expansion ability of a substance when heat is applied due to atoms' motion. Fig. 7a displays variation in thermal expansion with temperature for both hydrides. From this Figure, it is clear that α increases rapidly up to 400 K and then a sluggish increase can be seen as temperature increases. The increase in α at low temperature follows the T^3 rule [44].

Grüneisen parameters (γ) of hydrides are also obtained using the quasi-harmonic approximation. γ describes the anharmonic impact on the vibrating lattice and can be used to predict a substance's anharmonic properties. Grüneisen parameters of hydrides are illustrated in Fig. 7b. As Fig. 7b displays that Grüneisen parameters of hydrides demonstrate small change with temperature. It is also worthwhile to notice that γ differs from zero at 0 K, demonstrating that thermal expansion coefficient and specific heat capacity approaches zero in the same asymptotic way. In general, γ at 0 K is proportional to the logarithmic derivative of T^3 coefficient in the heat capacity with respect to volume [45].

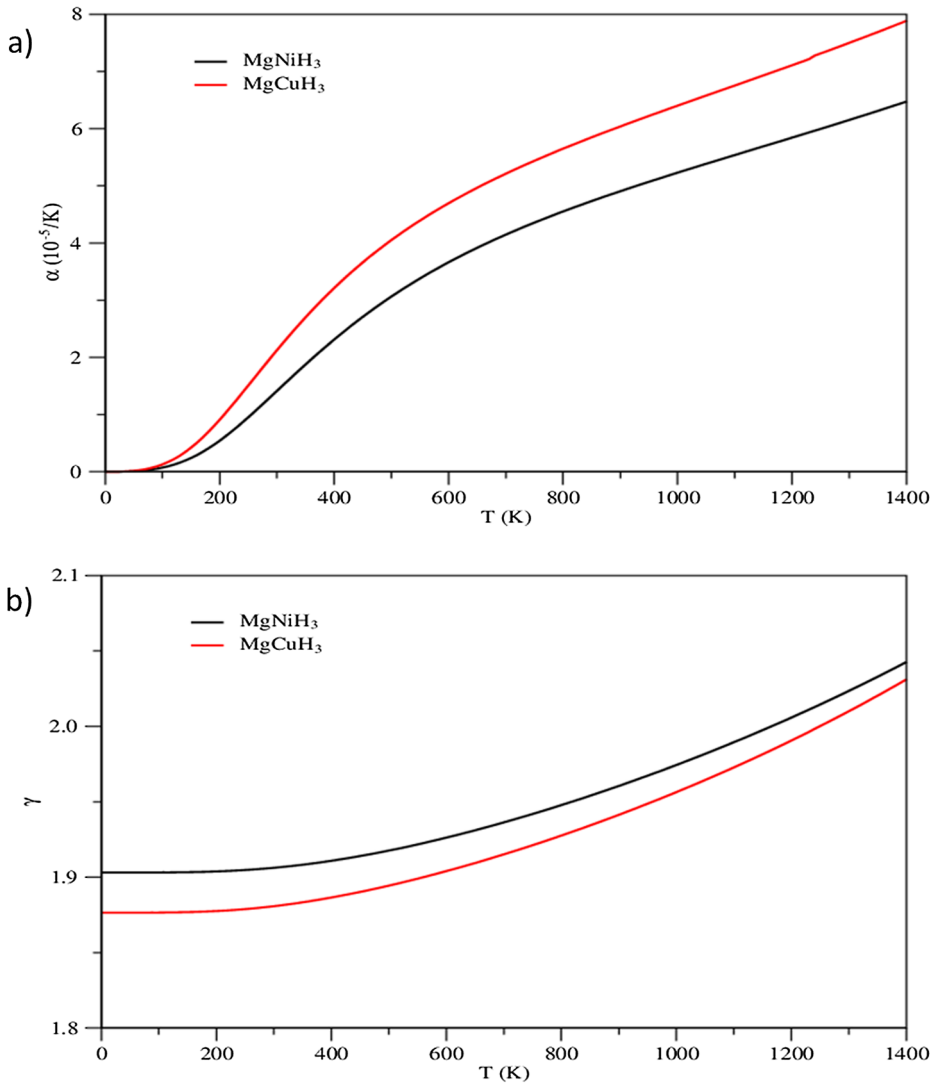

Fig. 7. Variations of thermal expansion coefficient (a) and Grüneisen parameter (b) with temperature for $MgNiH_3$ and $MgCuH_3$.

4. Conclusion

Computation of structural, elastic, electronic and thermodynamic properties of perovskite type ternary hydrides for solid state storage of hydrogen has been carried out via first principle method. The obtained equilibrium lattice constants of both ternary hydrides are found to be in a great agreement with the previously reported experimental data. The three independent elastic constants and other computed data has been presented for the first time. By evaluation of elastic constants of hydrides based on well-known. Born stability criteria, it is found that both ternary hydrides are mechanically stable. The nature of hydrides are evaluated using Bulk and Shear modulus along with Cauchy Pressure. As Pugh criteria indicated that the ratio of both modulus is higher than 1.75 and Cauchy pressures are both positive, which means that both ternary hydrides are ductile in nature. That is a wanted property for handling and transporting materials easily. The bonding analysis of hydrides revealed that both hydrides have dominant ionic bonding characteristics and central forces based on the Poisson‘s ratio. The compressibility of both hydrides are spherical whereas Poisson’s ratio, Shear and Young Modulus of $MgNiH_3$ and $MgCuH_3$ display a deviation from isotropy and becomes anisotropic at all directions. The electronic analysis proposed that both hydrides are metallic. Moreover, several thermodynamic characteristics such as Debye temperature, thermal expansion coefficient and specific heat values are reported. The results in this recent study are new and useful in terms of solid state hydrogen storage and serving as a reference data to literature.

Author contributions

We confirm that all authors contributed equally.

Declaration of Competing Interest

The authors declare that they have no known competing financial interests or personal relationships that could have appeared to influence the work reported in this paper.

References

[1] M. Abdellaoui, et al., The hydrogen storage properties of Mg-intermetallic-hydrides by ab initio calculations and kinetic Monte Carlo simulations, Int. J. Hydrogen Energy (2018).
[2] T. Vegge, et al., Trends in hydride formation energies for magnesium-3d transition metal alloys, J. Alloy. Compd. 386 (1) (2005) 1–7.
[3] K.F. Aguey-Zinsou, J.R. Ares-Fernandez, Hydrogen in magnesium: new perspectives toward functional stores, Energy Environ. Sci. 3 (5) (2010) 526–543.
[4] J.-C. Crivello, et al., Mg-based compounds for hydrogen and energy storage, Appl. Phys. A 122 (2) (2016) 85.
[5] S. Orimo, H. Fujii, Materials science of Mg-Ni-based new hydrides, Appl. Phys. A 72 (2) (2001) 167–186.
[6] G. Lefevre, et al., Hydrogen storage in MgX (X = Cu and Ni) systems - is there still

news? J. Power Sources 402 (2018) 394–401.
[7] G. Friedlmeier, et al., Preparation and structural, thermal and hydriding characteristics of melt-spun Mg–Ni alloys, J. Alloy. Compd. 292 (1) (1999) 107–117.
[8] J.P. Lei, et al., Synthesis and thermodynamic evaluation of intermetallic Mg-Ni/Mg-Cu nanoscale powders, J. Mater. Res. 24 (8) (2009) 2503–2510.
[9] M.X. Tanaka, et al., Effect of Ball-Milling on the Properties of Mg_2Cu Hydrogen Storage Alloy, Mater. Trans. 49 (11) (2008) 2698–2701.
[10] J. Iturbe-García, et al., Hydrogen desorption process in Mg_2Ni hydrides, Revista mexicana de física 52 (4) (2006) 365–367.
[11] K. Komiya, et al., Synthesis and decomposition of perovskite-type hydrides, $MMgH_3$ (M = Na, K, Rb), J. Alloy. Compd. 453 (1) (2008) 157–160.
[12] P. Vajeeston, et al., First-principles investigations of the $MMgH_3$ (M = Li, Na, K, Rb, Cs) series, J. Alloy. Compd. 450 (1) (2008) 327–337.
[13] M.A. Ghebouli, et al., Structural, elastic, electronic, optical and thermodynamic properties of $KMgH_3$, Solid State Sci. 13 (3) (2011) 647–652.
[14] M. Fornari, A. Subedi, D.J. Singh, Structure and dynamics of perovskite hydrides $AMgH_3$ (A = Na, K, Rb) in relation to the corresponding fluorides: A first-principles study, Phys. Rev. B 76 (21) (2007) 214118.
[15] P. Hohenberg, W. Kohn, Inhomogeneous Electron Gas, Phys. Rev. 136 (3B) (1964) B864–B871.
[16] W. Kohn, L.J. Sham, Self-consistent equations including exchange and correlation effects, Phys. Rev. 140 (4A) (1965) A1133–A1138.
[17] G. Paolo, et al., Quantum Espresso: a modular and open-source software project for quantum simulations of materials, J. Phys.: Condens. Matter 21 (39) (2009) 395502.
[18] J.P. Perdew, K. Burke, M. Ernzerhof, Generalized Gradient Approximation Made Simple, Phys. Rev. Lett. 77 (18) (1996) 3865–3868.
[19] K.F. Garrity, et al., Pseudopotentials for high-throughput DFT calculations, Comput. Mater. Sci. 81 (2014) 446–452.
[20] M. Methfessel, A. Paxton, High-precision sampling for Brillouin-zone integration in metals, Phys. Rev. B 40 (6) (1989) 3616.
[21] S. Baroni, P. Giannozzi, A. Testa, Green's-function approach to linear response in solids, Phys. Rev. Lett. 58 (18) (1987) 1861–1864.
[22] S. Baroni, et al., Phonons and related crystal properties from density-functional perturbation theory, Rev. Mod. Phys. 73 (2) (2001) 515–562.
[23] S. Al, Investigations of Physical Properties of XTiH3 and Implications for Solid State Hydrogen Storage, in: Zeitschrift für Naturforschung A. 2019, pp. 1023.
[24] A. Iyigor, Investigations of structural, elastic, electronic, vibrational and thermodynamic properties of RhMnX (X = Sb and Sn), Mater. Res. Express 6 (11) (2019) 116110.
[25] R. Singh, First principle study of structural, electronic and thermodynamic behavior of ternary intermetallic compound: CeMgTl, J. Magnesium Alloys 2 (4) (2014) 349–356.
[26] F.D. Murnaghan, The Compressibility of Media under Extreme Pressures, PNAS 30 (9) (1944) 244–247.
[27] S.F. Matar, A.F. Al Alam, N. Ouaini, Hydrogen insertion effects on the electronic structure of equiatomic MgNi traced by ab initio calculations, Zeitschrift für Naturforschung B 68 (1) (2013) 44–50.
[28] S. Al, N. Arikan, A. Iyigör, Investigations of Structural, Elastic, Electronic and Thermodynamic Properties of X_2TiAl Alloys: A Computational Study, Zeitschrift für Naturforschung A 73 (9) (2018) 859–867.
[29] A.H. Reshak, et al., First-principles calculations of structural, elastic, electronic, and optical properties of perovskite-type $KMgH_3$ crystals: novel hydrogen storage material, J. Phys. Chem. B 115 (12) (2011) 2836–2841.
[30] S. Benlamari, et al., Structural, electronic, elastic, and thermal properties of $CaNiH_3$ perovskite obtained from first-principles calculations, Chin. Phys. B 27 (3) (2018) 037104.
[31] S. Al, Theoretical investigations of elastic and thermodynamic properties of $LiXH_4$ compounds for hydrogen storage, Int. J. Hydrogen Energy 44 (3) (2019) 1727–1734.
[32] P. Li, et al., First-principles investigations on structural stability, elastic and electronic properties of Co_7M_6 (M = W, Mo, Nb) μ phases, Mol. Simul. 45 (9) (2019) 752–758.
[33] S.F. Pugh, XCII. Relations between the elastic moduli and the plastic properties of polycrystalline pure metals, Philosoph. Mag. J. Sci. 45 (367) (1954) 823–843.
[34] C. Kürkçü, Ç. Yamçıçıer, Structural, electronic, elastic and vibrational properties of two dimensional graphene-like BN under high pressure, Solid State Commun. 303–304 (2019) 113740.
[35] N. Miao, et al., Theoretical investigation on the transition-metal borides with Ta_3B_4-type structure: A class of hard and refractory materials, Comput. Mater. Sci. 50 (4) (2011) 1559–1566.
[36] L. Liu, et al., First-principles investigations on structural and elastic properties of orthorhombic TiAl under pressure, Crystals 7 (4) (2017) 111.
[37] C. Kürkçü, Z. Merdan, Ç. Yamçıçıer, Pressure-induced phase transitions, electronic, elastic and vibrational properties of zinc oxide under high pressure, Indian J. Phys. 93 (8) (2019) 979–989.
[38] V.V. Bannikov, I.R. Shein, A.L. Ivanovskii, Electronic structure, chemical bonding and elastic properties of the first thorium-containing nitride perovskite $TaThN_3$. Physica status solidi, (RRL) – Rapid Res. Lett. 1 (3) (2007) 89–91.
[39] A. Gencer, G. Surucu, S. Al, $MgTiO_3H_x$ and $CaTiO_3Hx$ perovskite compounds for hydrogen storage applications, Int. J. Hydrogen Energy 44 (23) (2019) 11930–11938.
[40] J. Chang, et al., Structure and mechanical properties of tantalum mononitride under high pressure: A first-principles study, J. Appl. Phys. 112 (8) (2012) 083519.
[41] H. Ledbetter, A. Migliori, A general elastic-anisotropy measure, J. Appl. Phys. 100 (6) (2006) 063516.
[42] A. Marmier, et al., ElAM: A computer program for the analysis and representation of anisotropic elastic properties, Comput. Phys. Commun. 181 (12) (2010) 2102–2115.
[43] P.L.D. Alexis Thérèse Petit, Recherches sur quelques points importants de la Théorie de la Chaleur, Annales de Chimie et de Physique 10 (1819) 395–413.
[44] A.T. Petit, Dulong, Recherches Sur quelques points importans de la theorie de la chaleur, 1819.
[45] S. Wei, C. Li, M.Y. Chou, Ab initio calculation of thermodynamic properties of silicon, Phys. Rev. B 50 (19) (1994) 14587–14590.